

Projected Wavefunctions and High Temperature Superconductivity

Arun Paramekanti, Mohit Randeria and Nandini Trivedi

Department of Theoretical Physics, Tata Institute of Fundamental Research, Mumbai 400005, India

We study the Hubbard model with parameters relevant to the cuprates, using variational Monte Carlo with projected d -wave states. For doping $0 < x \lesssim 0.35$ we obtain a superconductor whose order parameter tracks the observed nonmonotonic $T_c(x)$. The variational parameter $\Delta_{\text{var}}(x)$ scales with the $(\pi, 0)$ “hump” and T^* seen in photoemission. Projection leads to incoherence in the spectral function and from the *singular* behavior of its moments we obtain the nodal quasiparticle weight $Z \sim x$ though the Fermi velocity remains finite as $x \rightarrow 0$. The Drude weight D_{low} and superfluid density are consistent with experiment and $D_{\text{low}} \sim Z$.

PACS numbers: 74.20.-z, 74.20.Fg, 74.25.-q, 74.72.-h

(May 8, 2019)

Strong correlations are essential to understand d -wave high temperature superconductivity in doped Mott insulators [1]. The no-double occupancy constraint arising from strong correlations has been treated within two complementary approaches. Within the gauge theory approach [2], which is valid at all temperatures, the constraint necessitates the inclusion of strong gauge fluctuations. Alternatively, the constraint can be implemented exactly at $T = 0$ using the variational Monte Carlo (VMC) method. Previous variational studies [3–6] have focussed primarily on the energetics of competing states.

In this letter, we revisit projected wavefunctions of the form proposed by Anderson in 1987 [1]. We compute physically interesting correlations using VMC and show that projection leads to loss of coherence. We obtain information about low energy excitations from the singular behavior of moments of the occupied spectral function. Remarkably, our results for various observables are in semi-quantitative agreement with experiments on the cuprates. We also make qualitative predictions for the doping (x) dependence of correlation functions in projected states (for $x \ll 1$) from general arguments which are largely independent of the detailed form of the wavefunction and the Hamiltonian.

We use the Hubbard Hamiltonian $\mathcal{H} = \mathcal{K} + \mathcal{H}_{\text{int}}$. The kinetic energy $\mathcal{K} = \sum_{\mathbf{k}, \sigma} \epsilon(\mathbf{k}) c_{\mathbf{k}\sigma}^\dagger c_{\mathbf{k}\sigma}$ with $\epsilon(\mathbf{k}) = -2t(\cos k_x + \cos k_y) + 4t' \cos k_x \cos k_y$ the dispersion on a square lattice with nearest (t) and next-near (t') hopping. The on-site repulsion is $\mathcal{H}_{\text{int}} = U \sum_{\mathbf{r}} n_{\uparrow}(\mathbf{r}) n_{\downarrow}(\mathbf{r})$ with $n_{\sigma}(\mathbf{r}) = c_{\sigma}^\dagger(\mathbf{r}) c_{\sigma}(\mathbf{r})$. We work in the strongly correlated regime where $J = 4t^2/U$, $t' \lesssim t \ll U$ near half filling: $n = 1 - x$ with the hole doping $x \ll 1$. We choose $t' = t/4$, $t = 300\text{meV}$ and $U = 12t$, so that $J = 100\text{meV}$ consistent with neutron data on cuprates.

We describe the ground state by the wavefunction

$$|\Psi_0\rangle = \exp(iS)\mathcal{P}|\Psi_{\text{BCS}}\rangle. \quad (1)$$

Here $|\Psi_{\text{BCS}}\rangle = \left(\sum_{\mathbf{k}} \varphi(\mathbf{k}) c_{\mathbf{k}\uparrow}^\dagger c_{-\mathbf{k}\downarrow}^\dagger\right)^{N/2} |0\rangle$ is the N -electron d -wave BCS wave function with $\varphi(\mathbf{k}) = v_{\mathbf{k}}/u_{\mathbf{k}} = \Delta_{\mathbf{k}}/[\xi_{\mathbf{k}} + \sqrt{\xi_{\mathbf{k}}^2 + \Delta_{\mathbf{k}}^2}]$. The two variational parameters

μ_{var} and Δ_{var} determine $\varphi(\mathbf{k})$ through $\xi_{\mathbf{k}} = \epsilon(\mathbf{k}) - \mu_{\text{var}}$ and $\Delta_{\mathbf{k}} = \Delta_{\text{var}}(\cos k_x - \cos k_y)/2$. The projector $\mathcal{P} = \prod_{\mathbf{r}} (1 - n_{\uparrow}(\mathbf{r})n_{\downarrow}(\mathbf{r}))$ in Eq. (1) eliminates all configurations with double occupancy, as appropriate for $U \rightarrow \infty$.

The unitary transformation $\exp(iS)$ includes double occupancy perturbatively in t/U [7]. The transformation $\exp(-iS)\mathcal{H}\exp(iS)$ is well known to lead to the tJ Hamiltonian [7]. We emphasize that our approach effectively transforms *all* operators, and not only \mathcal{H} . Using $\langle\Psi_0|\mathcal{Q}|\Psi_0\rangle = \langle\Psi_{\text{BCS}}|\mathcal{P}\tilde{\mathcal{Q}}\mathcal{P}|\Psi_{\text{BCS}}\rangle$ with $\tilde{\mathcal{Q}} = \exp(-iS)\mathcal{Q}\exp(iS)$, it follows that incorporating $\exp(iS)$ in the wavefunction (1) is equivalent to transforming $\mathcal{Q} \rightarrow \tilde{\mathcal{Q}}$ and working with fully projected states.

Using standard VMC techniques [8] we compute equal-time correlators in the state $|\Psi_0\rangle$. The two variational parameters are determined by minimizing $\langle\Psi_0|\mathcal{H}|\Psi_0\rangle/\langle\Psi_0|\Psi_0\rangle$ at each x . The doping dependence of the resulting $\Delta_{\text{var}}(x)$ is shown in Fig. 1(a). Varying input parameters in \mathcal{H} we find that the scale for Δ_{var} is mainly determined by $J = 4t^2/U$. We show below that Δ_{var} is *not* proportional to the SC order parameter, in contrast to BCS theory, and also argue that it is *not* equal to the spectral gap. On the other hand, we find that the optimal $\mu_{\text{var}}(x) \approx \mu_0(x)$, the chemical potential of *noninteracting* electrons described by \mathcal{K} . However, μ_{var} is quite different [9] from the chemical potential $\mu = \partial\langle\mathcal{H}\rangle/\partial N$, where $\langle\cdots\rangle$ denotes the expectation value in the optimal, normalized ground state.

Phase Diagram: We now show that the wavefunction (1) is able to describe three phases: a resonating valence bond (RVB) insulator, a d -wave SC and a Fermi liquid metal. To establish the $T = 0$ phase diagram we first study off-diagonal long range order (ODLRO) using $F_{\alpha,\beta}(\mathbf{r} - \mathbf{r}') = \langle c_{\uparrow}^\dagger(\mathbf{r}) c_{\downarrow}^\dagger(\mathbf{r} + \hat{\alpha}) c_{\downarrow}(\mathbf{r}') c_{\uparrow}(\mathbf{r}' + \hat{\beta}) \rangle$, where $\hat{\alpha}, \hat{\beta} = \hat{x}, \hat{y}$. We find that $F_{\alpha,\beta} \rightarrow \pm\Phi^2$ for large $|\mathbf{r} - \mathbf{r}'|$, with $+$ ($-$) sign obtained for $\hat{\alpha} \parallel$ (\perp) to $\hat{\beta}$, indicating d -wave SC. As seen from Fig. 1(b) the order parameter $\Phi(x)$ is *not* proportional to $\Delta_{\text{var}}(x)$, and is nonmonotonic. Φ vanishes linearly in x as $x \rightarrow 0$ as first noted in ref. [4], even though $\Delta_{\text{var}} \neq 0$. We argue [10] that $\Phi \sim x$ is a general property of projected SC wavefunctions. The lo-

cal fixed number constraint imposed by \mathcal{P} at $x = 0$ leads to large quantum phase fluctuations that destroy SC order. The non-SC state at $x = 0$ is an insulator with a vanishing Drude weight, as shown below. The system is a SC in the doping range $0 < x < x_c \simeq 0.35$ with $\Phi \neq 0$. For $x > x_c$, $\Phi = 0$ and the wavefunction Ψ_0 for $\Delta_{\text{var}} = 0$ describes a normal Fermi liquid. In the remainder of this paper we will study $0 \leq x \leq x_c$.

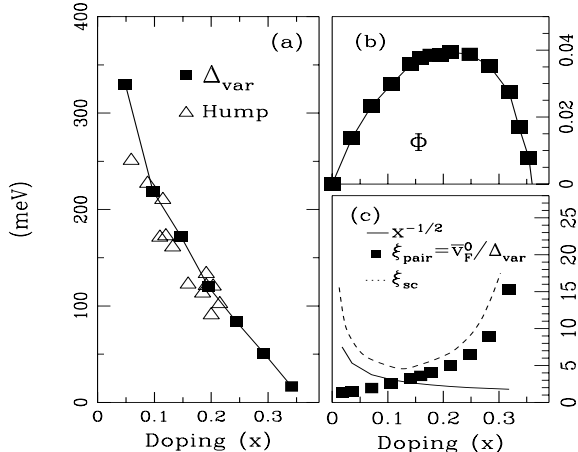


FIG. 1. (a): The variational parameter Δ_{var} (filled squares) and the $(\pi, 0)$ hump scale (open triangles) in ARPES [11] versus doping. (b): Doping dependence of the d -wave SC order parameter Φ . Solid lines in (a) and (b) are guides to the eye. (c): The coherence length $\xi_{\text{sc}} \geq \max(\xi_{\text{pair}}, 1/\sqrt{x})$.

Coherence Lengths: We must carefully distinguish between various ‘coherence lengths’, which are the same in BCS theory, but are very different in strongly correlated SC’s. The internal pair wavefunction $\varphi(\mathbf{k})$ defines a pair-size $\xi_{\text{pair}} \sim \bar{v}_F^0/\Delta_{\text{var}}$, where \bar{v}_F^0 is the bare average Fermi velocity. Projection does not affect the pair-size much, and ξ_{pair} remains finite at $x = 0$, where it defines the range of singlet bonds in the RVB insulator [1].

A second important length scale is the inter-hole spacing $1/\sqrt{x}$. At shorter distances there are no holes and the system effectively looks like the $x = 0$ insulator. Thus the superconducting coherence length ξ_{sc} must necessarily satisfy $\xi_{\text{sc}} \geq \max(\xi_{\text{pair}}, 1/\sqrt{x})$. This bound implies that ξ_{sc} must diverge both in the insulating limit $x \rightarrow 0$ (see also Refs. [2]) and the metallic limit $x \rightarrow x_c^-$, but is small at optimality; see Fig. 1(c). This non-monotonic behavior of $\xi_{\text{sc}}(x)$ should be checked experimentally.

Momentum Distribution: From gray-scale plots like Fig. 2 we see considerable structure in the momentum distribution $n(\mathbf{k})$ over the entire range $0 \leq x \leq x_c$. One cannot define a Fermi surface (FS) since the system is a SC (or an insulator). Nevertheless, for all x , the \mathbf{k} -space loci (i) on which $n(\mathbf{k}) = 1/2$ and (ii) on which $|\nabla_{\mathbf{k}} n(\mathbf{k})|$ is maximum, are both quite similar to the corresponding noninteracting FS’s. For $t' = t/4$, the FS is hole-like for $x \lesssim 0.22$, and electron-like for overdoping [12].

We next exploit the fact that moments of dynamical

cal correlations can be expressed as equal-time correlators, calculable in our formalism. Specifically, we look at $M_\ell(\mathbf{k}) = \int_{-\infty}^{\infty} d\omega \omega^\ell f(\omega) A(\mathbf{k}, \omega)$, where $A(\mathbf{k}, \omega)$ is the one-particle spectral function and, at $T = 0$, $f(\omega) = \Theta(-\omega)$. We calculate $M_0(\mathbf{k}) = n(\mathbf{k})$ and the first moment [13] $M_1(\mathbf{k}) = \langle c_{\mathbf{k}\sigma}^\dagger [\mathcal{H}, c_{\mathbf{k}\sigma}] \rangle$ to obtain important information about the spectral function.

Nodal Quasiparticles: Fig. 2(c) shows that along $(0, 0)$ to (π, π) $n(\mathbf{k})$ has a jump discontinuity. This implies the existence of gapless quasiparticles (QPs) observed by angle resolved photoemission spectroscopy (ARPES) [14]. The spectral function along the diagonal thus has the low energy form: $A(\mathbf{k}, \omega) = Z\delta(\omega - \tilde{\xi}_k) + A_{\text{inc}}$, where $\tilde{\xi}_k = v_F(k - k_F)$ is the QP dispersion and A_{inc} the smooth incoherent part. We estimate the nodal $k_F(x)$ from the location of the discontinuity and the QP weight Z from its magnitude. While $k_F(x)$ has weak doping dependence, $Z(x)$ is shown in Fig. 2(d), with $Z \sim x$ as the insulator is approached [15].

Projection leads to a suppression of Z from unity with the incoherent weight $(1 - Z)$ spread out to high energies. We infer large incoherent linewidths as follows. (a) At the ‘band bottom’ $n(\mathbf{k} = (0, 0)) \simeq 0.85$ (for $x = 0.18$) implying that 15% of the spectral weight must have spilled over to $\omega > 0$. (b) Even at k_F , the first moment M_1 lies significantly below $\omega = 0$ (defined by the chemical potential $\mu = \partial\langle\mathcal{H}\rangle/\partial N$); see Fig. 3(a).

The moments are dominated by the high energy incoherent part of $A(\mathbf{k}, \omega)$, but their *singular behavior is determined by the gapless coherent* QPs. Specifically, along the zone diagonal $M_1(\mathbf{k}) = Z\tilde{\xi}_k\Theta(-\tilde{\xi}_k) + \text{smooth part}$. Thus its slope $dM_1(\mathbf{k})/dk$ has a discontinuity of Zv_F at k_F , as seen in Fig. 3(a), and may be used to estimate [16] the nodal Fermi velocity v_F . As seen from Fig. 3(b), $v_F(x)$ is reduced from its bare value v_F^0 and is weakly doping dependent, consistent with the ARPES estimate [14] of $v_F \approx 1.5\text{eV}\cdot\text{\AA}$ in $\text{Bi}_2\text{Sr}_2\text{CaCu}_2\text{O}_{8+\delta}$ (BSCCO).

As $x \rightarrow 0$, $Z = [1 - \partial\Sigma'/\partial\omega]^{-1} \sim x$, while $v_F(x)/v_F^0 = Z[1 + (v_F^0)^{-1}\partial\Sigma'/\partial k]$ is weakly x -dependent. This implies a $1/x$ divergence in the \mathbf{k} -dependence of the self energy Σ on the zone diagonal, which could be tested by ARPES.

Within slave boson mean field theory (MFT) [1], we find [9] $Z^{\text{sb}} = x$ in Fig. 2(d) and $v_F^{\text{sb}}(x)$ shown in Fig. 3(b), both systematically smaller than the corresponding VMC results. Thus the holons and spinons must be partially bound by gauge fluctuations beyond MFT.

Moments Along $(\pi, 0) \rightarrow (\pi, \pi)$: The moments $n(\mathbf{k})$ and $M_1(\mathbf{k})$ near $\mathbf{k} = (\pi, 0)$ are not sufficient to estimate the SC gap, however they give insight into the nature of the spectral function. As seen from Fig. 4(a) $n(\mathbf{k})$ is much broader than that for the unprojected $|\Psi_{\text{BCS}}\rangle$. For \mathbf{k} ’s near (π, π) , which correspond to high energy, unoccupied ($\omega > 0$) states in $|\Psi_{\text{BCS}}\rangle$ we see a significant build up of spectral weight transferred from $\omega < 0$. Correspondingly, we see loss of spectral weight near $(\pi, 0)$. We thus infer large linewidths at all \mathbf{k} ’s, also seen from the large $|M_1(\mathbf{k})|$ (in Fig. 4(b)) relative to the BCS result.

The transfer of weight over large energies inferred above suggests that projection pushes spectral weight to $|\omega| < \Delta_{\text{var}}$, the gap in unprojected BCS theory. We thus expect that the true spectral gap $E_{\text{gap}} < \Delta_{\text{var}}$ and that the coherent QP near $(\pi, 0)$ must then reside at E_{gap} in order to be stable against decay into incoherent excitations. It is then plausible that Δ_{var} , the large gap before projection, is related to an incoherent feature in $A(\mathbf{k}, \omega)$ near $(\pi, 0)$ after projection [17]. Indeed, comparing Δ_{var} with the $(\pi, 0)$ “hump” feature seen in ARPES [11], we find good agreement in the magnitude as well as doping dependence; see Fig. 1(a).

Optical spectral weight: The optical conductivity sum rule states that $\int_0^\infty d\omega \text{Re}\sigma(\omega) = \pi \sum_{\mathbf{k}} m^{-1}(\mathbf{k}) n(\mathbf{k}) \equiv \pi D_{\text{tot}}/2$ where $m^{-1}(\mathbf{k}) = (\partial^2 \epsilon(\mathbf{k}) / \partial k_x \partial k_x)$ is the noninteracting mass tensor (we set $\hbar = c = e = 1$). The total optical spectral weight $D_{\text{tot}}(x)$ is plotted in Fig. 5(a) and seen to be non-zero even at $x = 0$, since the infinite cutoff in the integral above includes contributions from the “upper Hubbard band”.

A physically more interesting quantity is the *low frequency* optical weight, or Drude weight, D_{low} where the upper cutoff extends above the scale of t and J , but is much smaller than U . This is conveniently defined [9] by the response to an external vector potential: $D_{\text{low}} = \partial^2 \langle \mathcal{H}_A \rangle_A / \partial A^2$. Here the subscript on \mathcal{H} denotes that A enters the kinetic energy via a Peierls minimal coupling, and that on the expectation value denotes the corresponding modification of $\exp(iS)$ in Eq. (1). The Drude weight $D_{\text{low}}(x)$, plotted in Fig. 5(a), vanishes linearly as $x \rightarrow 0$, which can be argued to be a general property of projected states [9]. This also proves, following Ref. [18], that $|\Psi_0\rangle$ describes an insulator at $x = 0$. Both the magnitude and doping dependence of $D_{\text{low}}(x)$ are consistent with optical data on the cuprates [19].

Motivated by our results on the nodal $Z(x)$ and $D_{\text{low}}(x)$, we make a parametric plot of these two quantities in Fig. 5(b) and find that $D_{\text{low}} \sim Z$ over the entire doping range, a prediction which can be checked by comparing optics and ARPES [20] on the cuprates.

Superfluid Density: The Kubo formula for the superfluid stiffness D_s can be written as $D_s = D_{\text{low}} - \Lambda^T$, where D_{low} is the diamagnetic response, and Λ^T is the transverse current-current correlator. Using the spectral representation for Λ^T it is easy to see that [21] $\Lambda^T \geq 0$ implying $D_s \leq D_{\text{low}}$. Two conclusions follow. First, $D_s \rightarrow 0$ as $x \rightarrow 0$, consistent with experiments [22]. Second, we obtain a lower bound on the penetration depth λ_L defined by $\lambda_L^{-2} \equiv 4\pi e^2 D_s / \hbar^2 c^2 d_c$. Using the calculated $D_{\text{low}} \approx 90 \text{ meV}$ at optimality and a mean inter-layer spacing $d_c = 7.5 \text{ \AA}$ (appropriate to BSCCO), we find $\lambda_L \gtrsim 1350 \text{ \AA}$, consistent with experiment [23].

Conclusions: We have shown, within our variational scheme, the $T = 0$ evolution of the system from an undoped insulator to a d-wave SC to a Fermi liquid as a function of x . The SC order parameter $\Phi(x)$ is non-monotonic with a maximum at optimal doping $x \simeq 0.2$,

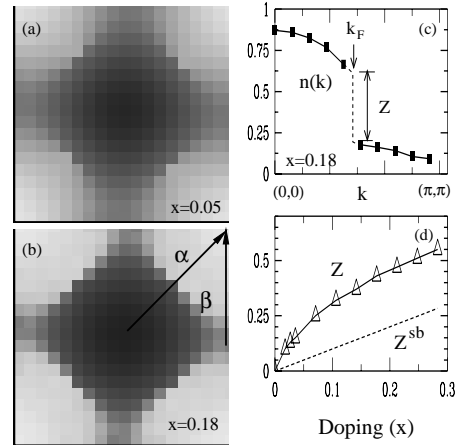


FIG. 2. (a) and (b): Gray-scale plots of $n(\mathbf{k})$ (black $\equiv 1$, white $\equiv 0$) centered at $\mathbf{k} = (0, 0)$ for $x = 0.05$ and $x = 0.18$ respectively on a $19 \times 19 + 1$ lattice, showing very little doping dependence of the large “Fermi surface”. (c): $n(\mathbf{k})$ plotted along the diagonal direction (indicated as α in Panel (b)), showing the jump at k_F which implies a gapless nodal quasiparticle of weight Z . (d): Nodal quasiparticle weight $Z(x)$, compared with the slave boson mean field $Z^{\text{sb}}(x)$ (dashed line).

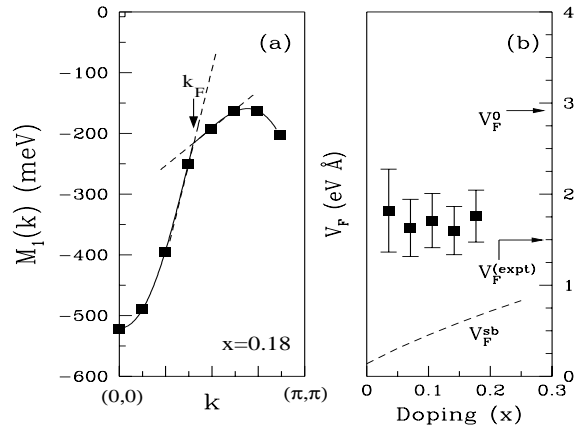


FIG. 3. (a): The moment $M_1(\mathbf{k})$ along the zone diagonal, with smooth fits for $k < k_F$ and $k > k_F$, showing a discontinuity of Zv_F in its slope at k_F . (b): Doping dependence of the nodal quasiparticle velocity obtained from $M_1(\mathbf{k})$. Error bars come from fits to $M_1(\mathbf{k})$ and errors in Z . Also shown are the bare nodal velocity v_F^0 , the slave boson mean field $v_F^{\text{sb}}(x)$ (dashed line), and the ARPES estimate $v_F^{(\text{expt})}$ [14].

suggestive of the experimental trend in $T_c(x)$ from under- to over-doping. As $x \rightarrow 0$ D_s vanishes, while the spectral gap, expected to scale with Δ_{var} , remains finite. Thus the underdoped state, with strong pairing and weak phase coherence, should lead to pseudogap behavior in the temperature range between T_c (which scales like Φ) and T^* (which scales like Δ_{var}).

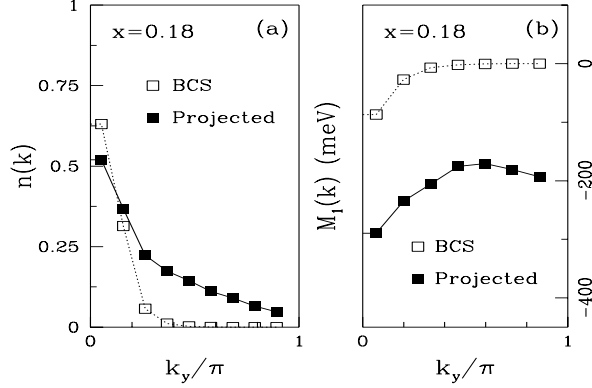


FIG. 4. (a): $n(\mathbf{k})$ plotted along the $(\pi, 0)$ - (π, π) direction (indicated as β in Fig. 2(b)) and compared with the BCS result. (b): The moment $M_1(\mathbf{k})$ plotted along the $(\pi, 0)$ - (π, π) direction compared with the BCS values.

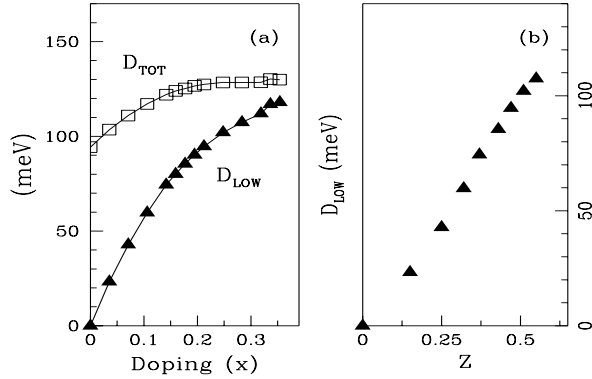


FIG. 5. (a): Doping dependence of the total (D_{tot}) and low energy (D_{low}) optical spectral weights (b): The optical spectral weight D_{low} versus the nodal quasiparticle weight Z .

Acknowledgements: We thank H.R. Krishnamurthy, P.A. Lee, M.R. Norman and J. Orenstein for helpful comments on an earlier draft. M.R. was supported in part by the DST through the Swarnajayanti scheme.

[1] P.W. Anderson, Science **235**, 1196 (1987); G. Baskaran, Z. Zou and P.W. Anderson, Sol. St. Comm. **63**, 973 (1987); G. Kotliar and J. Liu, Phys. Rev. B **38**, 5142 (1988).
[2] X. G. Wen and P. A. Lee, Phys. Rev. Lett. **78**, 4111 (1997); D. H. Lee, Phys. Rev. Lett. **84**, 2694 (2000).

[3] C. Gros, R. Joynt and T.M. Rice, Z. Phys. B **68**, 425 (1987); E.S. Heeb and T.M. Rice, Europhys. Lett. **27**, 673 (1994).
[4] C. Gros, Phys. Rev. B **38**, 931 (1988).
[5] H. Yokoyama and H. Shiba, J. Phys. Soc. Jpn. **57**, 2482 (1988); H. Yokoyama and M. Ogata, J. Phys. Soc. Jpn. **65**, 3615 (1996).
[6] F. Becca, M. Capone, and S. Sorella, Phys. Rev. B **62**, 12700 (2000).
[7] C. Gros, R. Joynt and T.M. Rice, Phys. Rev. B **36**, 381 (1987); A.H. MacDonald, S.M. Girvin and D. Yoshioka, Phys. Rev. B **37**, 9753 (1988).
[8] Since the pair wavefunction $\varphi(\mathbf{k})$ is singular on the zone diagonal we use “tilted” lattices [3] with periodic boundary conditions. Most results were obtained on a $15 \times 15 + 1$ site lattice, with some on a $19 \times 19 + 1$ lattice. Typically we used 5000 equilibration sweeps, and averaged over 500-1000 configurations from 5000 sweeps. In all the VMC results presented here, the error bars are of the size of the symbol, unless explicitly shown.
[9] Details will be presented in a longer paper; A. Paramekanti, M. Randeria and N. Trivedi (unpublished).
[10] To put a pair of electrons on a link near \mathbf{r} , after removing them from a link near the origin, requires two vacancies near \mathbf{r} . Thus $F_{\alpha, \alpha}(\mathbf{r}) \sim x^2$ and $\Phi \sim x$ as $x \rightarrow 0$.
[11] J-C. Campuzano *et al.*, Phys. Rev. Lett. **83**, 3709 (1999).
[12] A. Ino *et al.*, cond-mat/0005370.
[13] The Fourier transform of $M_1(\mathbf{k})$ is $M_1(\mathbf{r} - \mathbf{r}') = -t_{\mathbf{r}\mathbf{r}'} \langle c_{\sigma}^{\dagger}(\mathbf{r}) c_{\sigma}(\mathbf{r}') \rangle + U \langle c_{\sigma}^{\dagger}(\mathbf{r}) c_{\sigma}(\mathbf{r}') n_{\bar{\sigma}}(\mathbf{r}') \rangle$. Since the second term is $\mathcal{O}(U)$ we need S in Eq. (1) to $\mathcal{O}(t/U)^2$ to obtain $M_1(\mathbf{k})$ correctly to $\mathcal{O}(J)$.
[14] A. Kaminski *et al.*, Phys. Rev. Lett. **84**, 1788 (2000); and Phys. Rev. Lett. **86**, 1070 (2001).
[15] Relating Z to the amplitude of the asymptotic power-law decay in $\langle c_{\sigma}^{\dagger}(\mathbf{r}) c_{\sigma}(\mathbf{r}') \rangle$ we can show that $Z \sim x$ for projected states [9].
[16] For unprojected BCS wavefunctions we can estimate v_F with 5% accuracy using this method on finite systems.
[17] Numerically $|M_1(\pi, 0) - M_1(k_F^{\text{node}})| \sim \Delta_{\text{var}}$ for all x .
[18] A.J. Millis and S.N. Coppersmith, Phys. Rev. B **42**, 10807 (1990) and Phys. Rev. B **43**, 13770 (1991).
[19] Using a lattice spacing $a = 3.85 \text{ \AA}$ for BSCCO we find $(\omega_p^*)^2 \equiv (4\pi e^2/a) D_{\text{low}} \approx (1.8 \text{ eV})^2$ at optimal doping, in good agreement with data summarized in S.L. Cooper *et al.*, Phys. Rev. B **47**, 8233 (1993).
[20] D.L. Feng *et al.*, Science **280**, 277 (2000) and H. Ding *et al.*, cond-mat/0006143, find that the *anti*-nodal quasiparticle weight scales with the superfluid density.
[21] A. Paramekanti, N. Trivedi and M. Randeria, Phys. Rev. B **57**, 11639 (1998).
[22] Y.J. Uemura *et al.*, Phys. Rev. Lett. **62**, 2317 (1989).
[23] The agreement with the measured $\lambda \simeq 2100 \text{ \AA}$ in optimal BSCCO [S.F. Lee *et al.*, Phys. Rev. Lett. **77**, 735 (1996)] would be improved by including the effects of long wavelength quantum phase fluctuations; see A. Paramekanti *et al.*, Phys. Rev. B **62**, 6786 (2000), L. Benfatto *et al.*, cond-mat/0008100.